Hindawi Publishing Corporation
Mathematical Problems in Engineering
Volume 2013, Article ID 749689, 9 pages
http://dx.doi.org/10.1155/2013/749689

Research Article

Spatial Path Following for AUVs Using Adaptive Neural Network Controllers

Jiajia Zhou, Zhaodong Tang, Honghan Zhang, and Jianfang Jiao

College of Automation, Harbin Engineering University, Harbin 150001, China

Correspondence should be addressed to Zhaodong Tang; bsa323@163.com

Received 18 August 2013; Accepted 8 October 2013

Academic Editor: Hamid Reza Karimi

The spatial path following control problem of autonomous underwater vehicles (AUVs) is addressed in this paper. In order to realize AUVs' spatial path following control under systemic variations and ocean current, three adaptive neural network controllers which are based on the Lyapunov stability theorem are introduced to estimate uncertain parameters of the vehicle's model and unknown current disturbances. These controllers are designed to guarantee that all the error states in the path following system are asymptotically stable. Simulation results demonstrated that the proposed controller was effective in reducing the path following error and was robust against the disturbances caused by vehicle's uncertainty and ocean currents.

1. Introduction

The research of AUV has been a hot topic in recent years with the development of marine robotics. Voluminous literature, for example [1–3], has been presented on the subject of designing path following controllers for AUVs. In order to design an automatic path following control system for AUVs, several problems must be solved. Among them the most difficult and challenging is that AUV's dynamics are highly nonlinear and the hydrodynamic coefficients of vehicles are difficult to be accurately estimated a priori since the variations of these coefficients with different operating conditions. In addition to vehicle dynamics, Caharija et al. [4] pointed out that the sea currents affect the vehicles significantly which are the lack of actuation in sway. As a universal phenomenon, the single AUV's spatial path following problem is a basis for formation coordinated control of multiple AUVs [5, 6].

Hereinabove, it is shown that modelling inaccuracy is primary difficult to achieve oriented results. The data driven fault diagnosis and process monitoring methods based on input and output data could be an effective way in real-time implementation where the physical model is hard to obtain [7–9]. And when it comes to system uncertainty, robust control could be used to attenuate disturbances in a relatively suboptimal extent. For example, load disturbance in the modelling of vehicles could be restricted to a satisfied expectation using the robust H_∞ PID controller [10]. Compared with robust control theory, adaptive strategy is an effective method of dealing with optimal control problems in vehicle control systems [11, 12]. Wang et al. [13] designed an adaptive PID controller for the path tracking system. From the simulation results, it was known that the proposed controller could not satisfy the tracking characteristics during automation performance. Based on Lyapunov stability theory and backstepping, Lapierre and Soetanto [14] proposed a path following controller for the motion control system of an AUV. It was demonstrated that the control characteristics of this kind of controller was relied on the accuracy of the hydrodynamic model. Chen and Wang [15] presented an adaptive control law with a parameter projection mechanism to track the desired vehicle longitudinal motion in the presence of tire-road friction coefficient uncertainties and actively injected braking excitation signals. The simulation results demonstrated that the proposed method was valuable for autonomous vehicle systems. A parameter-dependent adaptive H_∞ controller was constructed in [16] to guarantee robust asymptotic stability of the linear parameter-varying systems. And numerical examples were carried out to verify the effective impact on the attenuation in system disturbance. Li et al. [17] found an adaptive controller using a new

neural network model, which was effective to improve the control precision by 30% in the case of system with random disturbance. To compensate the uncertainties in robot control systems, the radial basis functional (RBF) neural network was introduced to enhance system stability and transient performance [18].

In this paper, we propose an adaptive neural network control method for spatial path following control of an AUV. Three lightly interacting subsystems are introduced to fulfil this mission. RBF neural network (NN) is introduced to estimate unknown terms including inaccuracies of the vehicle. Adaptive laws are chosen to guarantee optimal estimation of the weight of NN to make the approximation more accurate. The control performance of the closed-loop systems are guaranteed by appropriately choosing the design parameters. Based on the Lyapunov stability theorem, the proposed controllers are designed to guarantee all the error states in the subcontrol systems which are asymptotically stable.

The paper is organized as follows. Section 2 formulates the vehicle dynamics for an underactuated AUV in the six-degree-of-freedom (6-DOF) form. Section 3 develops three adaptive neural network controllers to solve the path following problem with uncertain dynamics and external disturbance, such as sea currents. The proposed controllers' stability is analysed by Lyapunov theory in this section. The simulation results using the proposed controllers are illustrated in Section 4. Finally, Section 5 contains the main conclusions and describes some problems that warrant further investigation.

2. Problem Formulation

2.1. Vehicle Dynamics. The dynamic model of the AUV in the three dimensional space is described in this section. See details in Bian et al. [19]. The vehicle which we studied in this paper measures 7.45 × 2.32 × 1.97 m. It is equipped with two main thrusters for propulsion, which are mounted symmetrically about its longitudinal axis in the horizontal plane. A cruciform tail including two different control surfaces is fixed right behind the thrusters to provide an enlarged torque around the transverse axis in the body fixed frame, which is helpful in enhancing the ability of spatial path following control. This vehicle is underactuated for the lack of propellers about its normal axis and transverse axis. The maximum designed speed of the vehicle with respect to the water is 3.08 m/s approximately. An outline of the vehicle with respect to the earth-fixed coordinate and body-fixed coordinate is shown in Figure 1.

According to the criteria underwater vehicle motion model in Fossen [20], this 6-DOF model can be described as follows.

Dynamic equation:

$$\mathbf{M}\dot{\boldsymbol{\nu}} + \mathbf{C}(\boldsymbol{\nu})\boldsymbol{\nu} + \mathbf{D}(\boldsymbol{\nu})\boldsymbol{\nu} = \boldsymbol{\tau}. \tag{1}$$

Kinematic equation:

$$\dot{\boldsymbol{\eta}} = \mathbf{J}(\boldsymbol{\eta})\boldsymbol{\nu}, \tag{2}$$

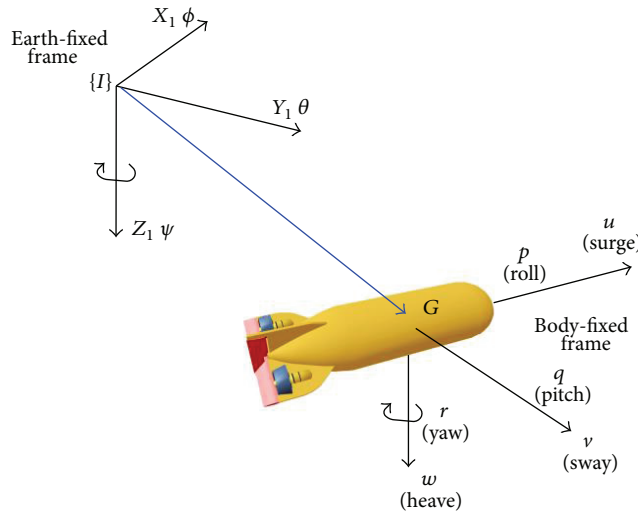

Figure 1: Employed coordinate frame systems.

where $\boldsymbol{\eta} = [\boldsymbol{\eta}_1, \boldsymbol{\eta}_2]^T$, $\boldsymbol{\nu} = [\boldsymbol{\nu}_1, \boldsymbol{\nu}_2]^T$, $\boldsymbol{\eta}_1 = [x, y, z]^T$, $\boldsymbol{\eta}_2 = [\varphi, \theta, \phi]^T$, $\boldsymbol{\nu}_1 = [u, v, w]^T$, and $\boldsymbol{\nu}_2 = [p, q, r]^T$.

The symbols φ, θ, ϕ, p, q, and r denote the roll, pitch, and yaw angles and velocities, respectively; x, y, z, u, v, and w are the surge, sway, and heave displacements and velocities, respectively. The matrix $\mathbf{J}(\boldsymbol{\eta}) = \text{diag}\{\mathbf{J}_1(\boldsymbol{\eta}_2), \mathbf{J}_2(\boldsymbol{\eta}_2)\}$ is the transformation matrix from the body-fixed coordinated frame to the earth-fixed coordinated frame; $\mathbf{M} = \mathbf{M}^T > 0$ is the mass and inertia matrix; $\mathbf{C}(\boldsymbol{\nu})$ is the Coriolis and centripetal matrix; $\mathbf{D}(\boldsymbol{\nu})$ is the damping matrix; $\boldsymbol{\tau}$ is the control input, including force and moments generated by propellers and hydroplanes.

2.2. Spatial Path Following. Spatial path following problems of AUV can be solved by a dynamic task and a geometric task, whose objectives are to make the vehicle sail at an expected speed and move to the proposed three-dimensional path.

The former process of path following problem can be briefly stated as follows. Given a spatial path Γ, the goal is to design some feedback control law which yields the control forces for the vehicle's thrusters so that its centre of mass would converge asymptotically to a desired path by forcing its speed to track a desired speed assignment. The latter one can be described as below: considering the AUV depicted in Figure 2, where P is an arbitrary point on the path and Q denotes its centre of mass. The objective is to design the controllers which force the vehicle's position to converge to the desired path by driving the course angle and depth to converge to desired ones.

3. Controller Design

The objective is to realize the path following for AUVs in three dimensions. Consider Healey and Lienard [21], and according to practical operational applications in AUVs, the 6-DOF nonlinear equations of motion can be separated into three lightly interacting subsystems, including diving,

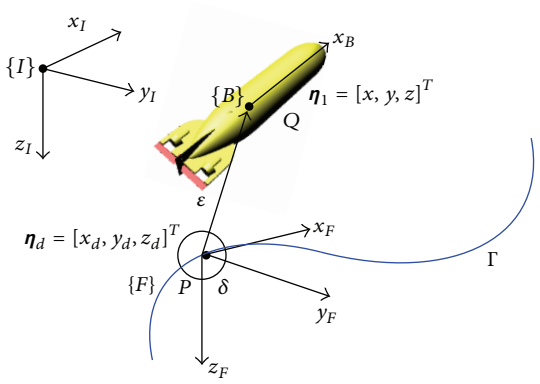

Figure 2: Spatial path following control problem.

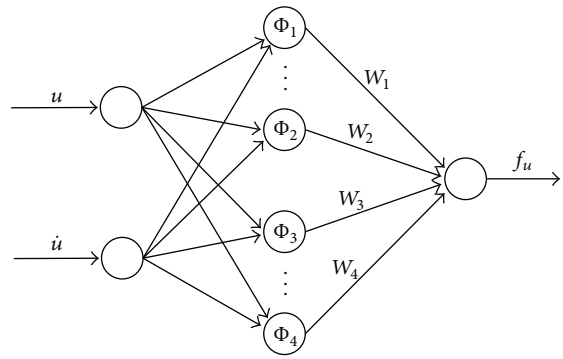

Figure 3: Diagram of RBF neural network for identification.

steering, and speed control. Our research will focus on dealing with the problem of spatial path following through the three subsystems.

3.1. Speed Control. For control design purposes, the interactions from the other degrees of freedom is neglected; the speed control model could be given by

$$\dot{u} = \frac{1}{(m - X_{\dot{u}})}\left[X_{uu}u^2 + X_{\text{prop}} + d_u\right], \tag{3}$$

where $X_{\dot{u}}$ and X_{uu} are dimensional hydrodynamic coefficients in surge; X_{prop} is thrusters' force; d_u represents modelling inaccuracies and external disturbances.

Define

$$f_u = X_{uu}u^2 + d_u. \tag{4}$$

Then, (4) can be rewritten as

$$\dot{u} = \frac{1}{(m - X_{\dot{u}})}\left(X_{\text{prop}} + f_u\right), \tag{5}$$

where X_{prop} is the forward force generated by the two main thrusters.

To deal with the uncertain terms, a RBF NN is chosen to estimate f_u which is described as

$$f_u = W_u^*\Phi_u + \varepsilon_u, \tag{6}$$

where W_u^* is an optimized weight estimation of the neural network; Φ_u is the basis function; ε_u is its estimation error. An identification diagram of the RBF neural network is shown in Figure 3.

Assume

$$X_{\text{prop}} = -\widehat{W}_u\Phi_u - k_u u, \tag{7}$$

where $k_u > 0$; $\widehat{W}_u$ is the weight estimation of the neural network.

Choose a Lyapunov function

$$V_u = \frac{1}{2}u^2 + \frac{1}{2}\widetilde{W}_u^2, \tag{8}$$

where $\widetilde{W}_u = W_u - \widehat{W}_u$.

Equation (8)'s derivative can be calculated as

$$\begin{aligned}\dot{V}_u &= u\dot{u} + \widetilde{W}_u\dot{\widetilde{W}}_u = u\dot{u} + \widetilde{W}_u\dot{\widetilde{W}}_u \\ &= u\left[\frac{X_{uu}u^2}{(m - X_{\dot{u}})} + \frac{X_{\text{prop}}}{(m - X_{\dot{u}})} + \frac{d_u}{(m - X_{\dot{u}})}\right] + \widetilde{W}_u\dot{\widetilde{W}}_u \\ &= \frac{u}{(m - X_{\dot{u}})}\left[X_{uu}u^2 + X_{\text{prop}} + d_u\right] + \widetilde{W}_u\dot{\widetilde{W}}_u \\ &= \frac{u}{(m - X_{\dot{u}})}\left[W_u\Phi_u + \varepsilon_u + X_{\text{prop}}\right] + \widetilde{W}_u\dot{\widetilde{W}}_u.\end{aligned} \tag{9}$$

Combined with (7) and (9),

$$\begin{aligned}\dot{V}_u &= \frac{u}{(m - X_{\dot{u}})}\left[W_u\Phi_u + \varepsilon_u - \widehat{W}_u\Phi_u - k_u u\right] + \widetilde{W}_u\dot{\widetilde{W}}_u \\ &= \frac{u\widetilde{W}_u\Phi_u}{(m - X_{\dot{u}})} + \frac{u\varepsilon_u}{(m - X_{\dot{u}})} - \frac{k_u u^2}{(m - X_{\dot{u}})} + \widetilde{W}_u\dot{\widetilde{W}}_u.\end{aligned} \tag{10}$$

An adaptive law is designed as follows:

$$\dot{\widetilde{W}}_u = \dot{\widetilde{W}}_u = -\frac{u\Phi_u}{(m - X_{\dot{u}})} + \lambda\left(\widehat{W}_u - W_{u0}\right), \tag{11}$$

where $\lambda_u > 0$; W_{u0} is the initial weight value of the neural network. Then (9) can be changed as

$$\begin{aligned}\dot{V}_u &= \frac{u\varepsilon_u}{(m - X_{\dot{u}})} - \frac{k_u u^2}{(m - X_{\dot{u}})} + \widetilde{W}_u\left(\frac{u\Phi_u}{(m - X_{\dot{u}})} + \dot{\widetilde{W}}_u\right) \\ &= \frac{u\varepsilon_u}{(m - X_{\dot{u}})} - \frac{k_u u^2}{(m - X_{\dot{u}})} + \widetilde{W}_u\lambda_u\left(\widehat{W}_u - W_{u0}\right).\end{aligned} \tag{12}$$

Because ε is small enough, $|u| < 3.1$ m/s, $m - X_{\dot{u}} \gg 0$, and $(u/(m - X_{\dot{u}}))\varepsilon$ can be considered as small positive constant.

In (12),

$$\begin{aligned}&\widetilde{W}_u\lambda_u\left(\widehat{W}_u - W_{u0}\right) \\ &\quad= \widetilde{W}_u\widehat{W}_u\lambda_u - \widetilde{W}_u W_{u0}\lambda_u \\ &\quad= -\frac{\lambda_u}{2}\left\|\widetilde{W}_u\right\|_F^2 - \frac{\lambda}{2}\left\|\widehat{W}_u - W_{u0}\right\|_F^2 \\ &\qquad+ \frac{\lambda_u}{2}\left\|W_u - W_{u0}\right\|_F^2.\end{aligned} \tag{13}$$

Based on Lyapunov stability theorem, it is provided that if one of the inequations in (14) is true, (15) would come true which guarantees the speed error converge to a small neighbourhood zero domain.

$$\begin{aligned} \frac{\lambda_u}{2}\left\|\widetilde{W}_u\right\|_F^2 &\geq \frac{\lambda_u}{2}\left\|W_u - W_{u0}\right\|_F^2, \\ \frac{\lambda_u}{2}\left\|\widehat{W}_u - W_{u0}\right\|_F^2 &\geq \frac{\lambda_u}{2}\left\|W_u - W_{u0}\right\|_F^2, \end{aligned} \tag{14}$$

$$\dot{V}_u \leq -\gamma_u V_u + \sigma_u, \tag{15}$$

where $\gamma_u > 0$; σ_u is a small positive constant.

3.2. Diving Control. Consider the vehicle dynamics referred in Silvestre and Pascoal [22], and for the sake of diving control design, it is defined as follows:

$$\begin{aligned} dz &= -u_0(\theta - \sin\theta) + (u_0 - u)\sin\theta \\ &\quad + w\cos\theta, \\ b &= \left(I_y - \frac{1}{2}\rho L^5 M'_{\dot{q}}\right)^{-1}, \\ f_q &= b\left[\frac{1}{2}\rho L^5 M'_{q|q|}q\,|q| + \frac{1}{2}\rho L^4 M'_{uq}uq \right. \\ &\quad \left. + \frac{1}{2}\rho L^3 M'_{uu}u^2\right], \\ M_{Ty} &= \frac{1}{2}\rho L^3 M'_{\delta s}u^2\delta_s. \end{aligned} \tag{16}$$

If the surge speed is $u = u_0$, the depth control model can be simplified as

$$\begin{aligned} \dot{z} &= -u_0\theta + dz, \\ \dot{\theta} &= q, \\ \dot{q} &= f_q + bM_{Ty}, \\ Y &= z. \end{aligned} \tag{17}$$

To be convenient for controller design, (17) can be rewritten as

$$\begin{bmatrix} \dot{\varsigma}_1 \\ \dot{\varsigma}_2 \\ \dot{\varsigma}_3 \\ Y \end{bmatrix} = \begin{bmatrix} \varsigma_2 + d\varsigma_1 \\ \varsigma_3 \\ -u_0 f_q + \left(-u_0 b M_{Ty}\right) \\ \varsigma_1 \end{bmatrix} = \begin{bmatrix} f(\varsigma_1, \varsigma_2) \\ f_2(\varsigma_3) \\ f_3 - b' M_{Ty} \\ \varsigma_1 \end{bmatrix}, \tag{18}$$

where $\varsigma = [\varsigma_1, \varsigma_2, \varsigma_3]^T = [z, -u_0\theta, -u_0 q]^T$.

In this section the backstepping techniques are adopted based on iterative methodology, where a virtual control input is introduced to ensure that the diving error can be converged to zero. And based on the Lyapunov stability theorem, an adaptive neural network controller is designed to guarantee that all the error states in the diving control system are asymptotically stable.

From (18), a more simplified pure-feedback form is shown as follows:

$$\begin{bmatrix} \dot{\varsigma}_1 \\ \dot{\varsigma}_2 \\ \dot{\varsigma}_3 \end{bmatrix} = \begin{bmatrix} f(\varsigma_1, \varsigma_2) \\ f_2(\varsigma_3) \\ f_3 - b' M_{Ty} \end{bmatrix}. \tag{19}$$

Step 1. Given a desired depth ς_{d1}, the depth error is described as

$$\begin{aligned} \dot{Z}_1 &= \varsigma_1 - \varsigma_{d1} \\ &= f_1(\varsigma_1, \varsigma_2, u) - \dot{\varsigma}_{d1}. \end{aligned} \tag{20}$$

Define a virtual control variable:

$$\nu_1 = -\varsigma_{d1} + K_1 \dot{Z}_1. \tag{21}$$

From $\partial\nu_1/\partial\varsigma_2 = 0$, we can know

$$\frac{\partial\left[f_1(\varsigma_1, \varsigma_2, u) + \nu_1\right]}{\partial\varsigma_2} > \varepsilon > 0. \tag{22}$$

When we take ς_2 as the input of the virtual control variable, there must exist a $\varsigma_2 = \alpha_1^*(\varsigma_1, \nu_1, u)$ satisfying

$$f_1(\varsigma_1, \alpha_1^*, u) + \nu_1 = 0. \tag{23}$$

Referring to the mean value theorem of Lagrange, γ_1 $(0 < \gamma_1 < 1)$ can be found which yields

$$f_1(\varsigma_1, \varsigma_2, u) = f_1(\varsigma_1, \alpha_1^*, u) + \gamma_1(\varsigma_2, \alpha_1^*), \tag{24}$$

where $\gamma_1 := g_1(\varsigma_1, \varsigma_{2\gamma_1}, u)$, $\varsigma_{2\gamma_1} = \gamma_1\varsigma_2 + (1 - \gamma_1)\alpha_1^*$.

Combined with (21) and (24), (20) can be rewritten as

$$\dot{Z}_1 = -K_1 Z_1 + \gamma_1(\varsigma_2 - \alpha_1^*). \tag{25}$$

Then α_1^* can be estimated by RBF neural network as follows:

$$\alpha_1^* = W^{*T}\Phi(Z_1) + \varepsilon. \tag{26}$$

Consider $Z_2 = \varsigma_2 - \alpha_1$ and $\alpha_1 = -c_1 Z_1 + \widehat{W}^T\Phi(Z_1)$, where $\widehat{W}$ is to be the estimation of W^*. Then (25) becomes

$$\begin{aligned} \dot{Z}_1 &= -K_1 Z_1 + \gamma_1(Z_2 + \alpha_1 - \alpha_1^*) \\ &= -K_1 Z_1 + \gamma_1\left[Z_2 - c_1 Z_1 + \widetilde{W}^T\Phi(Z_1) - \varepsilon\right], \end{aligned} \tag{27}$$

where $\widetilde{W} = \widehat{W} - W^*$.

Choose a Lyapunov function:

$$V_1 = \frac{1}{2\gamma_1}Z_1^2 + \frac{1}{2}\widetilde{W}^T\Gamma_1\widetilde{W}. \tag{28}$$

The derivative of (28) can be calculated as

$$\dot{V}_1 = -\frac{K_1}{\gamma_1}Z_1^2 + Z_1Z_2 - c_1Z_1^2 - \frac{\gamma_1}{2\gamma_1^2}Z_1^2 - Z_1\varepsilon + \widetilde{W}^T\Phi(Z_1)Z_1 + \widetilde{W}^T\Gamma_1\widetilde{W}. \tag{29}$$

With the adaptive law,

$$\dot{\widehat{W}} = \left[-\Phi(Z_1)Z_1 - \sigma_1\left(\widehat{W}\right)\right]\cdot\Gamma_1, \tag{30}$$

where σ is a small positive constant.

Step 2. Consider

$$Z_2 = \varsigma_2 - \alpha_1 \Longrightarrow \dot{Z}_2 = f_2(\varsigma_3) = \varsigma_3. \tag{31}$$

It is assumed that

$$\alpha_2 = -Z_1 - c_2Z_2 + \alpha_1^*. \tag{32}$$

Choose another Lyapunov function:

$$V_2 = V_1 + \frac{1}{2}Z_2^2. \tag{33}$$

The derivative of (33) can be calculated as

$$\dot{V}_2 = -\frac{K_1}{\gamma_1}Z_1^2 - c_1Z_1^2 - \frac{\sigma\left\|\widetilde{W}\right\|^2}{2} + \frac{\sigma\|W^*\|^2}{2} + \frac{\varepsilon^2}{4c_1} - c_2Z_2^2 + Z_2Z_3. \tag{34}$$

Step 3. Define $\varsigma_3 = Z_3 - \alpha_2$.

It can be calculated as

$$\dot{Z}_3 = f_q - b'M_{Ty} - \dot{\alpha}_2. \tag{35}$$

And, we can obtain

$$M_{Ty}^* = -Z_2 - c_3Z_3 - \frac{1}{b'}\left(\dot{\alpha}_2 - f_q\right). \tag{36}$$

Then the unknown term $(1/b')f_q$ can be estimated by RBF NN, and the ideal optimal control law can be written as

$$M_{Ty}^* = -Z_2 - c_3Z_3 + W_2^*\Phi(Z_3) - \frac{\dot{\alpha}_2}{b'} + \varepsilon_2. \tag{37}$$

Finally, we obtain the actual control input:

$$M_{Ty} = -Z_2 - c_3Z_3 - \frac{\dot{\alpha}_2}{b'} + \widehat{W}_2\Phi(Z_3). \tag{38}$$

From (35)–(37), it can be derived that

$$\dot{Z}_3 = -K_3Z_3 - b'\left[-Z_2 - c_3Z_3 - \frac{\dot{\alpha}_2}{b'} + \widetilde{W}_2^T\Phi(Z_3) - \varepsilon_2\right]. \tag{39}$$

Consider a Lyapunov function:

$$V_3 = V_2 - \frac{1}{2b'}Z_3^2 + \frac{1}{2}\widetilde{W}_2^T\Gamma_2\widetilde{W}_2. \tag{40}$$

We can obtain its derivative

$$\dot{V}_3 = V_2 - Z_2Z_3 - c_3Z_3^2 + \widetilde{W}_2\Phi(Z_3)Z_3 + \widetilde{W}_2^T\Gamma_2\dot{\widehat{W}}_2, \tag{41}$$

where $\dot{\widehat{W}}_2 = \Gamma_2[-\Phi(Z_3)Z_3 - \sigma_3\widehat{W}_2]$ and $\sigma_3 > 0$.

As what we did in Step 1, (41) can be calculated as

$$\dot{V}_3 < -\sum_{j=1}^{3}c_{j0}^*Z_j^2 - \sum_{j=1}^{3}\frac{\sigma_j\left\|\widehat{W}_j\right\|}{2} + \sum_{j=1}^{3}\frac{\sigma_j\left\|W_j^*\right\|}{2} + \sum_{j=1}^{3}\frac{\varepsilon_j}{2}, \tag{42}$$

where $c_{30}^* := c_{30} > 0$.

Consider the Lyapunov stability theorem, it can be concluded that all the signals in the diving control system are bounded. Furthermore, the output tracking error of the system will converge to a small neighbourhood zero domain by appropriately choosing control parameters.

3.3. Guidance Law and Steering Control

3.3.1. Line-of-Sight Guidance. Referring to Fossen [20] and Oh and Sun [23], we briefly introduce Line-of-Sight guidance law in this section for path following in the horizontal plane and discuss its application for straight lines and circular arcs.

Calculate the angle between the proposed path and the north of earth-fixed coordinate in Figure 4:

$$\alpha_k := \arctan 2\left(\eta_{k+1} - \eta_k, \xi_{k+1} - \xi_k\right) \in [-\pi, \pi]. \tag{43}$$

Considering the cross track error $e_\gamma(t)$ and a look-ahead distance Δ, the desired course angle for the steering control system can be computed as

$$\gamma_d = \alpha_k + \arctan\left(\frac{-e_\gamma}{\Delta}\right) = \alpha_k + \gamma_e, \tag{44}$$

where $\Delta = nL$ ($n = 2\sim5$).

When it comes to the circular arcs in Figure 5, we can obtain the guidance law just as (44) in form.

3.3.2. Steering Controller Design. Referring to the vehicle dynamics in horizontal plane in [24] and considering the advantage of steering controller design, we define

$$X_1 = \psi, \qquad X_2 = \dot{\psi}. \tag{45}$$

The kinetics model of the AUV in horizontal plane can be simplified as

$$\begin{bmatrix}\dot{X}_1\\ \dot{X}_2\\ Y_\psi\end{bmatrix} = \begin{bmatrix}X_2\\ f_\psi(\upsilon) + b_\psi\delta_r + d_\psi\\ X_1\end{bmatrix}, \tag{46}$$

where $\upsilon := g_\psi(u, v, r)$ includes the nonlinear terms with u, v, and r in the steering equation; d_ψ is the disturbance satisfied with $|d_\psi| \le \varepsilon_0$, $\varepsilon_0 > 0$.

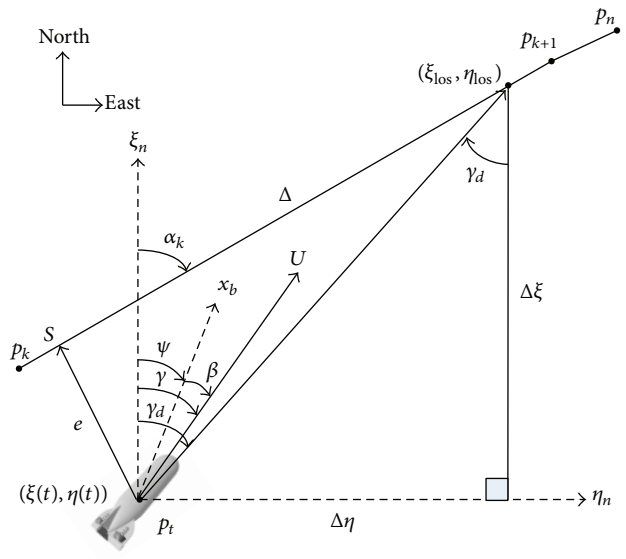

Figure 4: Principle of LOS guidance for straight line.

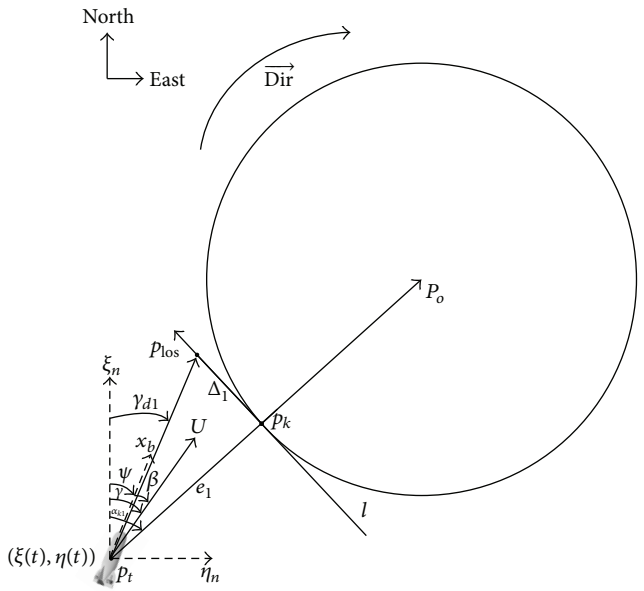

Figure 5: Principle of LOS guidance for circular arc.

Consider a heading track error:

$$e_\psi = Y_\psi - Y_{\psi d}, \tag{47}$$

where the desired course angle $\gamma_d = Y_{\psi d}$.

Choose $K \in R$ which makes (48) a stabilized system:

$$h(s) = s + K. \tag{48}$$

Then the derivative of the steering error system can be written as follows:

$$\dot{e}_\psi = \mathbf{A}e_\psi + \mathbf{B}\left[f_\psi(\upsilon) + b_\psi\tau - \ddot{Y}_{\psi d} + \mathbf{K}e_\psi + d_\psi\right], \tag{49}$$

where $A = -K$ and $B = 1$.

Then we can find $P > 0$ and $Q \geq 0$ which make the following Lyapunov stable equation solvable:

$$A^T P + PA = -Q. \tag{50}$$

On the assumption that $f_\psi(\upsilon)$ and b_ψ are known and $d_\psi = 0$, a linear controller can be obtained as (51) using pole-assignment method:

$$u_\psi = -b_\psi^{-1}\left(f_\psi(\upsilon) - \ddot{Y}_{\psi d} + \mathbf{K}e_\psi\right). \tag{51}$$

Combined with (46), we can find

$$\dot{e}_\psi + \mathbf{K}e_\psi = 0. \tag{52}$$

For K is chosen appropriately according to (48), it can be derived that $\lim_{t\to\infty} e_\psi(t) = 0$.

In fact, $f_\psi(\upsilon)$ and b_ψ are uncertain, and d_ψ does exist. To deal with the uncertain terms, a RBF NN is chosen to estimate $f_\psi(\upsilon)$:

$$f_\psi(\upsilon) = W^*\Phi(\upsilon) + \varepsilon_\psi, \tag{53}$$

where W^* is an optimized weight estimation of the neural network; $\Phi(\upsilon)$ is a vector of Gaussian function $\Phi(\upsilon) = \exp(\|\upsilon - c_0\|^2/{b_0}^2)$, $c_0 \in R$ is its centre, and b_0 is the width of the basis function.

If the weight estimation of neural network $\widehat{W}$ is uniformly bounded, a positive constant w can be found, which satisfies $\|\widehat{W}\| < w_0$.

For ε_ψ is the estimation error of the RBF NN, then

$$f_\psi(\upsilon) - \widehat{f}_\psi(\upsilon) = \varepsilon_\psi. \tag{54}$$

Meanwhile, consider a weight error for the RBF NN:

$$\widetilde{W} = W^* - \widehat{W}. \tag{55}$$

Combined with (49), (54), and (55), it can be calculated as

$$\begin{aligned}\dot{e}_\psi &= Ae_\psi + B\Big[\widehat{f}_\psi(\upsilon) + \widehat{b}_\psi\delta_r - \ddot{Y}_{\psi d} + Ke_\psi \\ &\quad + \left(f_\psi(\upsilon) - \widehat{f}_\psi(\upsilon)\right) \\ &\quad + \left(b_\psi - \widehat{b}_\psi\right)\delta_r + d_\psi(t)\Big] \\ &= Ae_\psi + B\Big[\widehat{f}_\psi(\upsilon) + \widehat{b}_\psi\delta_r - \dot{Y}_{\psi d} + Ke_\psi \\ &\quad + \Delta f_\psi + \widetilde{W}\phi(\upsilon) + \widetilde{b}_\psi\delta_r + d_\psi\Big].\end{aligned} \tag{56}$$

In order to compensate for estimation error and current disturbance as shown in (56), a virtual control input described as (17) is introduced as

$$\nu = -\kappa\frac{B^T P e_\psi}{\left\|B^T P e_\psi\right\| + \lambda_\psi}, \tag{57}$$

where $\kappa = P + \varepsilon_\psi$ and $\kappa \geq |\Delta f_\psi| + |d_\psi|$; λ_ψ is a small positive constant.

Herein, (56) can be rewritten as follows:

$$\dot{e}_\psi = Ae_\psi + B\left[\Delta f_\psi + \widetilde{W}\phi(\xi) + \tilde{b}_\psi \tau_\psi + d_\psi + \nu\right]. \quad (58)$$

Introduce adaptive laws:

$$\dot{\widetilde{W}} = \gamma_1 \Phi(\xi) BPe_\psi, \qquad \dot{\tilde{b}}_\psi = \gamma_2 \tau_\psi BPe_\psi, \quad (59)$$

where γ_1 and γ_2 are positive constants.

To deal with the problem of stability, a Lyapunov function (60) is chosen to guarantee the proposed adaptive NN controller satisfying that the signals in the steering control system are bounded:

$$V_\psi = \frac{1}{2}Pe_\psi^2 + \frac{1}{2\gamma_1}\widetilde{W}^2 + \frac{1}{2\gamma_2}\tilde{b}_\psi^2. \quad (60)$$

The differentiation of (60) can be calculated as

$$\begin{aligned}\dot{V}_\psi &= e_\psi \dot{e}_\psi P + \frac{1}{\gamma_1}\widetilde{W}\dot{\widetilde{W}} + \frac{1}{\gamma_2}\tilde{b}_\psi \dot{\tilde{b}}_\psi \\ &= e_\psi PB\left(\Delta f_\psi + d_\psi + \widetilde{W}\phi(\upsilon) + \tilde{b}_\psi \delta_s + \nu\right) \\ &\quad + \frac{1}{\gamma_1}\widetilde{W}\dot{\widetilde{W}} + \frac{1}{\gamma_2}\tilde{b}_\psi \dot{\tilde{b}}_\psi.\end{aligned} \quad (61)$$

With a combination of (59) and (61), it can be derived that

$$\dot{V}_\psi = e_\psi PB\left(\Delta f_\psi + d_\psi + \nu\right). \quad (62)$$

Moreover, because

$$\begin{aligned}&e_\psi^T PB\left(\Delta f_\psi + d_\psi + \nu\right) \\ &\le \left\|B^T Pe_\psi\right\|\left(\left\|\Delta f_\psi\right\| + \left\|d_\psi\right\|\right) + e_\psi^T PB\nu \\ &= \left\|B^T Pe_\psi\right\|\left(\left\|\Delta f_\psi\right\| + \left\|d_\psi\right\|\right) - \kappa\frac{\left(B^T Pe_\psi\right)^2}{\left\|B^T Pe_\psi\right\| + \lambda_\psi} \\ &\le \left\|B^T Pe_\psi\right\|\left(\left\|\Delta f_\psi\right\| + \left\|d_\psi\right\|\right) - \kappa\frac{\left\|B^T Pe_\psi\right\|^2}{\left\|B^T Pe_\psi\right\| + \lambda_\psi}\end{aligned} \quad (63)$$

and $\|B^T Pe_\psi\|^2/(\|B^T Pe_\psi\| + \lambda_\psi) > \|B^T Pe_\psi\| - \lambda_\psi$ are true, (62) can be calculated as

$$\dot{V}_\psi \le \left\|B^T Qe_\psi\right\|\left(\left\|\Delta f_\psi\right\| + \left\|d_\psi\right\| - \kappa\left\|B^T Pe_\psi\right\| - \lambda_\psi\right). \quad (64)$$

It is known that $\kappa \ge |\Delta f_\psi| + |d_\psi|$; then we can obtain

$$\dot{V}_\psi \le -\kappa\lambda_\psi \le 0. \quad (65)$$

Similar to the derivation of diving controller, it can be concluded that all the signals in the steering control system are bounded. Furthermore, the output tracking error of the system will converge to a small neighbourhood zero domain by appropriately choosing control parameters.

Finally, the control input can be given by

$$u_\psi = -\hat{b}_\psi^{-1}\left(\hat{f}_\psi(\upsilon) - \dot{Y}_{\psi d} + \mathbf{K}e_\psi - \nu\right). \quad (66)$$

4. Simulation Results

In order to validate the proposed controller, it is assessed in the C/C++ simulation environment with a full nonlinear model for the designed vehicle. It is assumed that the states of the system are updated with a period of $T = 0.1$ s (seconds). Considering jacket healthy state detection which is a regular task for offshore platform, a spiral three-dimensional path is programmed to complete the detection job. In order to fulfil this mission successfully, the control objective is going to achieve a high tracking precision with the proposed control method.

Two simulations are carried out to demonstrate the advantage of the proposed method, including path following conditions without sea current and undersea current, where the unvarying current is set to be heading east with 0.25 m/s. The vehicle is initially rest at a random position $(x, y, z) = (0\,\text{m}, 35\,\text{m}, 0.5\,\text{m})$ with an unspecified attitude $(\varphi, \theta, \psi) = (0^\circ, 0^\circ, 90^\circ)$. The desired forward speed is 1.8 m/s. The gains and parameters for the adaptive neural network speed controller are $\lambda_u = 1.2$, $k_u = 2.5$, and $\gamma_u = 1.8$, while the ANN steering controller's initial values are set as follows: $c_1 = 5$, $c_2 = 12$, $c_3 = 10$, $b = 3.8386e-005$, $\Gamma_1 = \Gamma_2 = \text{diag}\{1.5\}$, and $\sigma_1 = \sigma_3 = 0.5$. The parameters for the diving control system are chosen as $K = 2.8$, $\lambda_\psi = 0.1$, $\gamma_1 = 2$, and $\gamma_2 = 1.5$. And the initial weights of RBF NN for the three subsystems are chosen as zero.

Figures 6–9 show the simulation results for spatial path following between different ocean circumstances. It is shown that the proposed mission under disturbance of current or not could be achieved by the designed adaptive neural network controllers. It is clear that the proposed method is suitable to follow the spatial path with a random position and attitude, which is very practical in jacket healthy state detection mission.

Figure 6 is the response of spatial path following under different circumstances in three-dimensional space, where S means the start point and E is the end of the mission. We can see that the performances in the two simulations are good in general. It can be seen that the two tracks are identical with the same initial values for controllers' compensation to the uncertain dynamics and ocean current.

From Figure 7, it is shown that the position track errors during the jacket detection missions are gradually converged to zero. Combined with Figures 7 and 8, we can clearly see that although the overshoots have a little increase at the 67th second and the 54th one, which indicate the presence of ocean current in the process, the errors decrease to zero very quickly using the proposed controllers, which was designed to guarantee the errors in the spatial path following systems to be restricted to a small value gradually. In the meanwhile, when it is compared to the surge speed responses under different circumstances in Figure 9, it is evident that the fluctuant speed is the primary reason responsible for the overshoots in the spatial path following.

The simulation results obtained illustrate that the proposed methodology is effective and reduces the path following errors. Moreover, it is relatively simple to apply this proposed control in simulation.

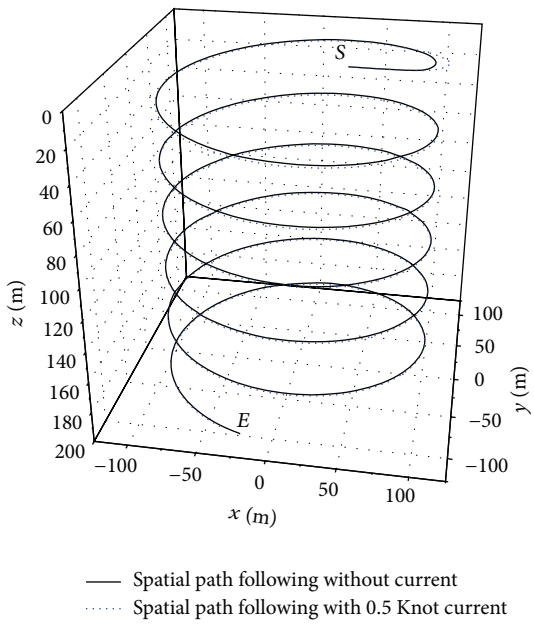

Figure 6: Spatial path following under different circumstances.

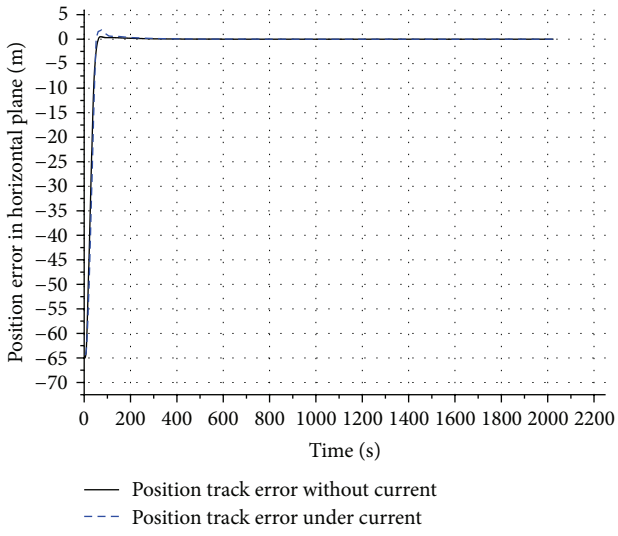

Figure 7: Position track errors in the horizontal plane.

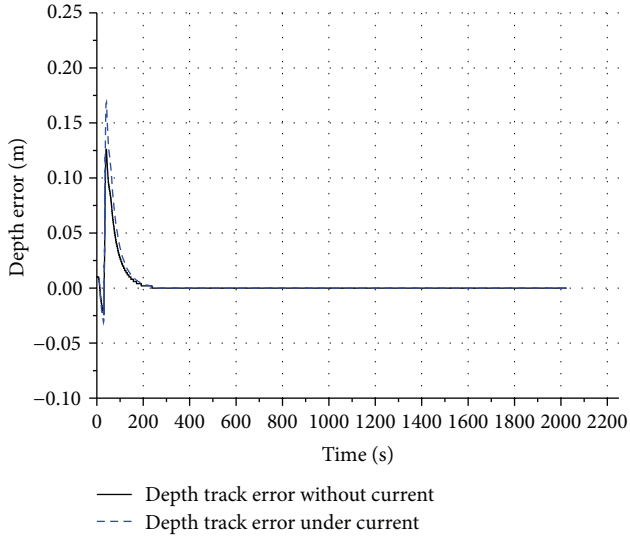

Figure 8: Depth track errors in the vertical plane.

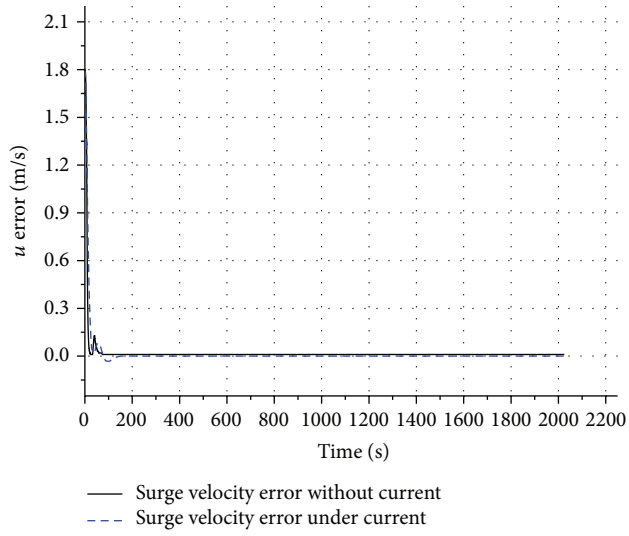

Figure 9: Surge speed errors under different circumstances.

5. Conclusions

The objective of this paper was to accurately follow a given path in the presence of systemic variations and ocean current. On one hand, three lightly interacting subsystems, including diving, steering, and speed control, were proposed to simplify the controller design for the spatial path following with 6-DOF nonlinear equations. On the other hand, those three controllers were designed to guarantee that all the error states in the spatial path following system were asymptotically stable by using adaptive neural network method. The simulation results illustrated that the proposed methodology was effective and attenuated the path following error under current. Future work will address the problems of path following under more common spatial curves. The problem of external disturbance about varying sea currents also warrants further research.

Acknowledgments

This work was supported by the Fundamental Research Funds for the Central Universities, under Grant HEUCF041330; the Fundamental Research Funds for the Central Universities of key laboratory's open key; the National Natural Science Foundation of China, under Grant 51309067/E091002. And the authors also would like to thank the editor and three reviewers for their helpful comments.

References

[1] P. Encarnação and A. Pascoal, "3D path following for autonomous underwater vehicle," in *Proceedings of the 39th IEEE Confernce on Decision and Control*, pp. 2977–2982, Sydney, Australia, December 2000.

[2] L. Lapierre and B. Jouvencel, "Robust nonlinear path-following control of an AUV," *IEEE Journal of Oceanic Engineering*, vol. 33, no. 2, pp. 89–102, 2008.

[3] H. M. Jia, L. J. Zhang, X. Q. Bian et al., "A nonlinear bottom-following controller for underactuated autonomous under water vehicles," *Journal of Central South University*, vol. 19, pp. 1240–1248, 2012.

[4] W. Caharija, K. Y. Pettersen, J. T. Gravdahl, and E. Borhaug, "Path following of underactuated autonomous underwater vehicles in the presence of ocean currents," in *Proceedings of the 51th IEEE Conference on Decision and Control*, pp. 528–535, Maui, Hawaii, USA, 2012.

[5] Y. Tang, H. J. Gao, W. Zou et al., "Distributed synchronization in networks of agent systems with nonlinearities and random switchings," *IEEE Transactions on Cybernetics*, vol. 43, no. 1, pp. 358–370, 2013.

[6] Y. Tang, H. J. Gao, J. Kurths et al., "Evolutionary pinning control and its application in UAV coordination," *IEEE Transactions on Industrial Informatics*, vol. 8, no. 4, pp. 828–838, 2012.

[7] S. Yin, S. Ding, and H. Luo, "Real-time implementation of fault tolerant control system with performance optimization," *IEEE Transactions on Industrial Electronics*, vol. 61, no. 5, pp. 2402–2411, 2013.

[8] S. Yin, S. Ding, A. Haghani et al., "A comparison study of basic data-driven fault diagnosis and process monitoring methods on the benchmark Tennessee Eastman process," *Journal of Process Control*, vol. 22, no. 9, pp. 567–1581, 2012.

[9] S. Yin, S. X. Ding, A. H. A. Sari, and H. Hao, "Data-driven monitoring for stochastic systems and its application on batch process," *International Journal of Systems Science*, vol. 44, no. 7, pp. 1366–1376, 2013.

[10] H. Zhang, Y. Shi, and A. S. Mehr, "Robust H_∞ PID control for networked control systems with acceptable noise rejection," in *Proceedings of the American Control Conference (ACC '10)*, pp. 1356–1361, Marriott Waterfront, Baltimore, Md, USA, July 2010.

[11] S. Yin, X. Yang, and H. R. Karimi, "Data-driven adaptive observer for fault diagnosis," *Mathematical Problems in Engineering*, vol. 2012, Article ID 832836, 21 pages, 2012.

[12] Y. Tang and W. K. Wong, "Distributed synchronization of coupled neural networks via randomly occurring control," *IEEE Transactions on Neural Networks and Learning Systems*, vol. 24, no. 3, pp. 435–447, 2013.

[13] B. Wang, Y. M. Su, L. Wan, and Y. Sun, "Adaptive PID control system for an autonomous underwater vehicle," *High Technology Letters*, vol. 17, no. 1, pp. 7–12, 2011.

[14] L. Lapierre and D. Soetanto, "Nonlinear path-following control of an AUV," *Ocean Engineering*, vol. 34, no. 11-12, pp. 1734–1744, 2007.

[15] Y. Chen and J. M. Wang, "Adaptive vehicle speed control with input injections for longitudinal motion independent road frictional condition estimation," *IEEE Transactions on Vehicular Technology*, vol. 60, no. 3, pp. 839–848, 2011.

[16] H. R. Karimi, "Parameter-dependent adaptive Hꝏ control design for a class of linear parameter-varying systems using polynomially parameter-dependent quadratic functions," *Proceedings of the Institution of Mechanical Engineers I*, vol. 221, no. 4, pp. 589–600, 2007.

[17] X. H. Li, F. Xu, J. H. Zhang et al., "A multilayer feed forward small-world neural network controller and its application on electrohydraulic actuation system," *Journal of Applied Mathematics*, vol. 2013, Article ID 872790, 8 pages, 2013.

[18] S. H. Wen, J. Y. Yuan, and J. H. Zhu, "Radial basis functional link network and Hamilton Jacobi Issacs for force/position control in robotic manipulation," *Mathematical Problems in Engineering*, vol. 2012, Article ID 568796, 10 pages, 2012.

[19] X. Q. Bian, C. H. Mou, Z. P. Yan, and H. Wang, "Formation coordinated control for multi-AUV based on spatial curve path tracking," in *Proceedings of the MTS/IEEE Kona Conference (OCEANS '11)*, Waikoloa, Hawaii, USA, September 2011.

[20] T. I. Fossen, *Handbook of Marine Craft Hydrodynamics and Motion Control*, John Wiley & Sons, New York, NY, USA, 2011.

[21] A. J. Healey and D. Lienard, "Multivariable sliding mode control for autonomous diving and steering of unmanned underwater vehicles," *IEEE Journal of Oceanic Engineering*, vol. 18, no. 3, pp. 327–339, 1993.

[22] C. Silvestre and A. Pascoal, "Depth control of the INFANTE AUV using gain-scheduled reduced order output feedback," *Control Engineering Practice*, vol. 15, no. 7, pp. 883–895, 2007.

[23] S.-R. Oh and J. Sun, "Path following of underactuated marine surface vessels using line-of-sight based model predictive control," *Ocean Engineering*, vol. 37, no. 2-3, pp. 289–295, 2010.

[24] C. Silvestre and A. Pascoal, "Control of the INFANTE AUV using gain scheduled static output feedback," *Control Engineering Practice*, vol. 12, no. 12, pp. 1501–1509, 2004.